

Part I: lithium metasilicate (Li_2SiO_3)—mild condition hydrothermal synthesis, characterization, and optical properties

Abdolali Alemi · Shahin Khademinia

Received: 17 July 2014 / Accepted: 29 October 2014 / Published online: 11 November 2014
© The Author(s) 2014. This article is published with open access at Springerlink.com

Abstract Using LiNO_3 and SiO_2 as raw materials, Li_2SiO_3 nano-powders were synthesized via a nonstoichiometric 2:3 Li:Si molar ratio hydrothermal reaction at 180 °C for 48, 72, and 96 h in a NaOH aqueous solution system. The synthesized materials were characterized by powder X-ray diffraction technique and Fourier transform infrared spectroscopy. To investigate the effect of the reaction time on the morphology of the obtained materials, the morphologies of the synthesized materials were studied by field emission scanning electron microscopy technique. The technique showed that on increasing the reaction time, the morphology of the as-prepared samples changed from belt structures to flower structures. Ultraviolet–Visible spectra analyses showed that the nanostructured lithium silicate powders had good light absorption properties in the ultraviolet light region. Also, photo luminescence spectra and cell parameter refinement of the obtained materials were studied.

Keywords Lithium metasilicate · Hydrothermal method · Nano materials · PXRD · SEM

Introduction

Silicates are the most abundant and most complicated class of minerals on earth with tremendous technological applications in fields such catalysis, microelectronics,

biomedicine, photonics, and traditional glass and ceramic industries [1]. In particular, the crystalline lithium silicates are present as important phases in silicate glass ceramics [2] and are of research interest because of their technological applications in areas such as CO_2 captures [3–9], lithium battery cathode materials [10], fast ion conductors [11], optical waveguides [12], and tritium breeding materials [13, 14]. Several groups have reported some methods to synthesize Li_2SiO_3 nanomaterials including solid state reaction, precipitation, sol–gel method, extrusion-spherodisation process, rotating/melting procedures, combustion, electrochemical method, and via hydrothermal method. However, most of the time, a mixture of Li_2SiO_3 , $\text{Li}_2\text{Si}_2\text{O}_5$, Li_4SiO_4 , and SiO_2 was obtained [10, 12, 15–21]. Recently, we have reported the synthesis of highly pure and crystalline lithium metasilicate nanomaterials through a mild condition hydrothermal method using lithium nitrate and silicic acid as raw materials at 1:2 Li:Si molar ratio [22, 25]. In the present study, a hydrothermal route was successfully explored to synthesize nanostructured Li_2SiO_3 powders in a hydrothermal system of LiNO_3 , SiO_2 , and NaOH. To the best of our knowledge, there is no report on the synthesis of nanostructured Li_2SiO_3 crystallites by these raw materials. The effects of reaction time on the final products in phase composition and particle morphology were investigated, and the band gap energy of the as-prepared Li_2SiO_3 samples was initially estimated from UV–Visible spectra. Besides, photo luminescence (PL) spectra and cell parameter refinement analysis were studied.

Materials and methods

All chemicals of analytical grade were obtained from commercial sources and were used without further

A. Alemi
Department of Inorganic Chemistry, Faculty of Chemistry,
University of Tabriz, Tabriz, Iran
e-mail: alemi.aa@gmail.com

S. Khademinia (✉)
Department of Chemistry, Semnan University, Semnan, Iran
e-mail: shahinkhademinia@gmail.com

purification. Phase identifications were performed on a powder X-ray diffractometer D5000 (Siemens AG, Munich, Germany) using Cu K α radiation. The morphology of the obtained materials was examined with a field emission scanning electron microscope (Hitachi FESEM model S-4160). Also, Fourier transform infrared (FTIR) spectra were recorded on a Tensor 27 (Bruker Corporation, Germany). Absorption and photoluminescence spectra were recorded on a Jena Analytik Specord 40 (AnalytikJena UK, Wembley, UK) and a PerkinElmer LF-5 spectrometer (PerkinElmer, Waltham, MA, USA), respectively. Also, cell parameter refinement was reported by celref software version 3.

Experimental

In a typical synthetic experiment, 0.400 g (5.80 mmol) of LiNO₃ (Mw = 68.95 gmol⁻¹) and 0.522 g (8.69 mmol) of SiO₂ (Mw = 60.08 gmol⁻¹) were added to 60 mL of hot aqueous solutions of 0.3 M NaOH under magnetic stirring at 80 °C. The resultant solution was further stirred for 15 min. Then, the solution was transferred into a 100-mL

Teflon-lined stainless steel autoclave. The autoclave was sealed and heated at 180 °C for 48 (sample 1) or 72 h (sample 2) or 96 h (sample 3). When the reaction was completed, it is cooled to room temperature by water immediately. The prepared powder was washed with distilled water and dried at 110 °C for 20 min under normal atmospheric conditions, and was allowed to cool slowly to room temperature to collect a white powder.

Result and discussion

Powder X-ray diffraction analysis

The crystal phases of the hydrothermally synthesized nanomaterials at 180 °C from 0.3 M NaOH solution with different reaction times for 48 (S₁), 72 (S₂) and 96 (S₃) h were examined by powder X-ray diffraction (PXRD) technique. As shown in Fig. 1, with the Li:Si molar ratio of 2:3 in the reaction mixture, a highly pure crystalline phase of Li₂SiO₃ (space group of Cmc2₁ [22–27]) was obtained after 48, 72, and 96 h. So, it shows that with lithium nitrate and SiO₂ as raw materials the main phase is lithium metasilicate. Compared to our another works using lithium carbonate and silicic acid at 2:3 Li:Si molar ratio at 180 °C for 72 h, the main phase was lithium metasilicate but the morphology of the obtained materials was flower structure [28]. Also, using lithium sulfate and silicic acid as raw materials at 2:3 Li:Si molar ratio at 180 °C for 48 and 72 h, the main phase was lithium sodium silicate nanostructures with straw bundle-like structure [29]. So, it shows that the raw material types at a certain Li:Si molar ratio are important factors on phase formation and morphology structure. A interplanar spacing (*d*) in the crystalline material is calculated via Bragg's equation ($n\lambda = 2d_{hkl} \sin\theta$). Thus compared to those of the like nanoparticles of pure lithium silicates, with increasing the reaction time, the diffraction lines in the powder XRD patterns of the nanoparticles of lithium metasilicate shift to a higher 2 θ values ($\Delta 2\theta = 26.86$ (96 h) – 26.81(48 h) = 0.05° and $\Delta d = 3.3283$ Å (48 h) – 3.3153 Å (96 h) = 0.013 Å. So, according to the above measurements, there is a contraction in the unit cell with changing the reaction time from 48 to 96 h. Also, the measured crystal sizes calculated by Scherrer equation summarized in Table 1 are in good

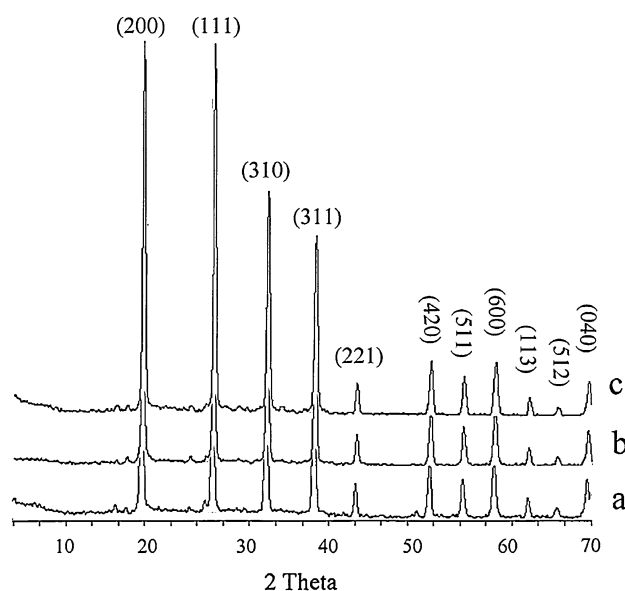


Fig. 1 PXRD patterns of the synthesized Li₂SiO₃ nanoparticles, where (a) is the synthesis at 48 h; (b) is the synthesis at 72 h; and (c) is the synthesis at 96 h at 180 °C

Table 1 Scherrer data information for pure Li₂SiO₃ nanomaterials obtained after 48, 72, and 96 h at 180 °C in 0.3 M NaOH solution

| Data information | 2 θ | θ value | B _{1/2} (°) | B _{1/2} (radian) | Cos θ_B | Crystal size (nm) |
|------------------|------------|----------------|----------------------|---------------------------|----------------|-------------------|
| Sample 1 | 26.81 | 13.405 | 0.288408 | 0.005031 | 0.97276 | 28.32 |
| Sample 2 | 26.81 | 13.405 | 0.284292 | 0.004959 | 0.97276 | 28.73 |
| Sample 3 | 26.86 | 13.430 | 0.309266 | 0.005395 | 0.97265 | 26.41 |

Fig. 2 FESEM images of the hydrothermally synthesized Li_2SiO_3 nanomaterials obtained after **a** 48 h at 180 °C

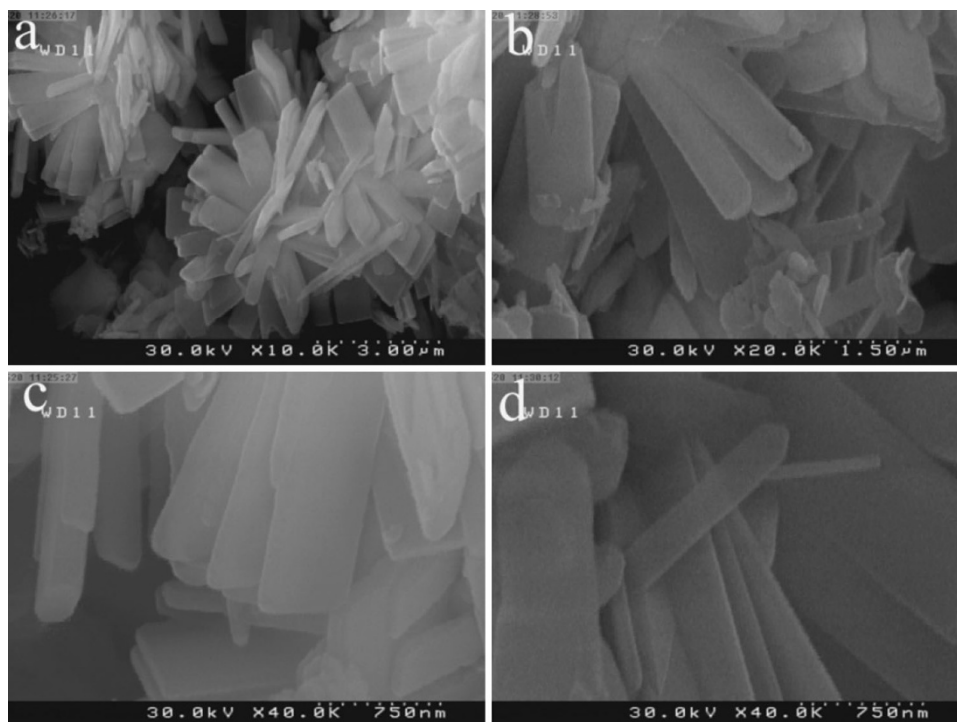
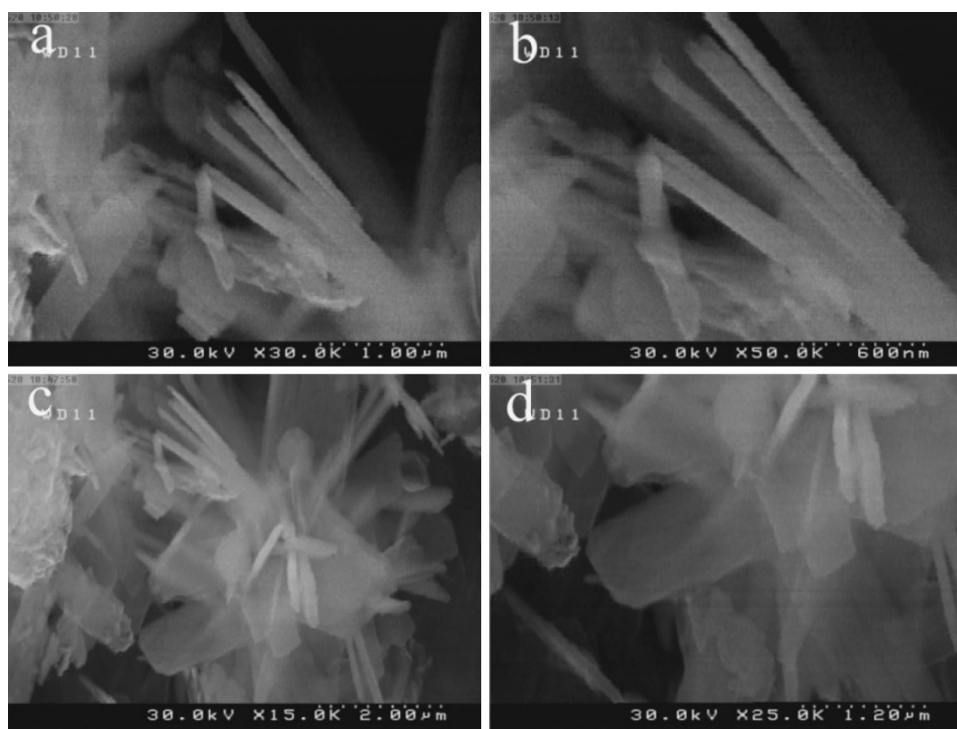


Fig. 3 FESEM images of the hydrothermally synthesized Li_2SiO_3 nanomaterials obtained after 72 h at 180 °C



agreement with interplanar spacing in the crystalline material measured via Bragg's equation.

Figure 2 shows typical field emission scanning electron microscopy (FESEM) images of the hydrothermally

synthesized Li_2SiO_3 nanomaterials after 48 h at 180 °C. From the typical FESEM images of S_1 , at low magnification in Fig. 2a, b and c, it is clear that the morphology of the obtained materials is nearly belt like and the belts have

Fig. 4 FESEM images of the hydrothermally synthesized Li_2SiO_3 nanomaterials obtained after 96 h at 180 °C

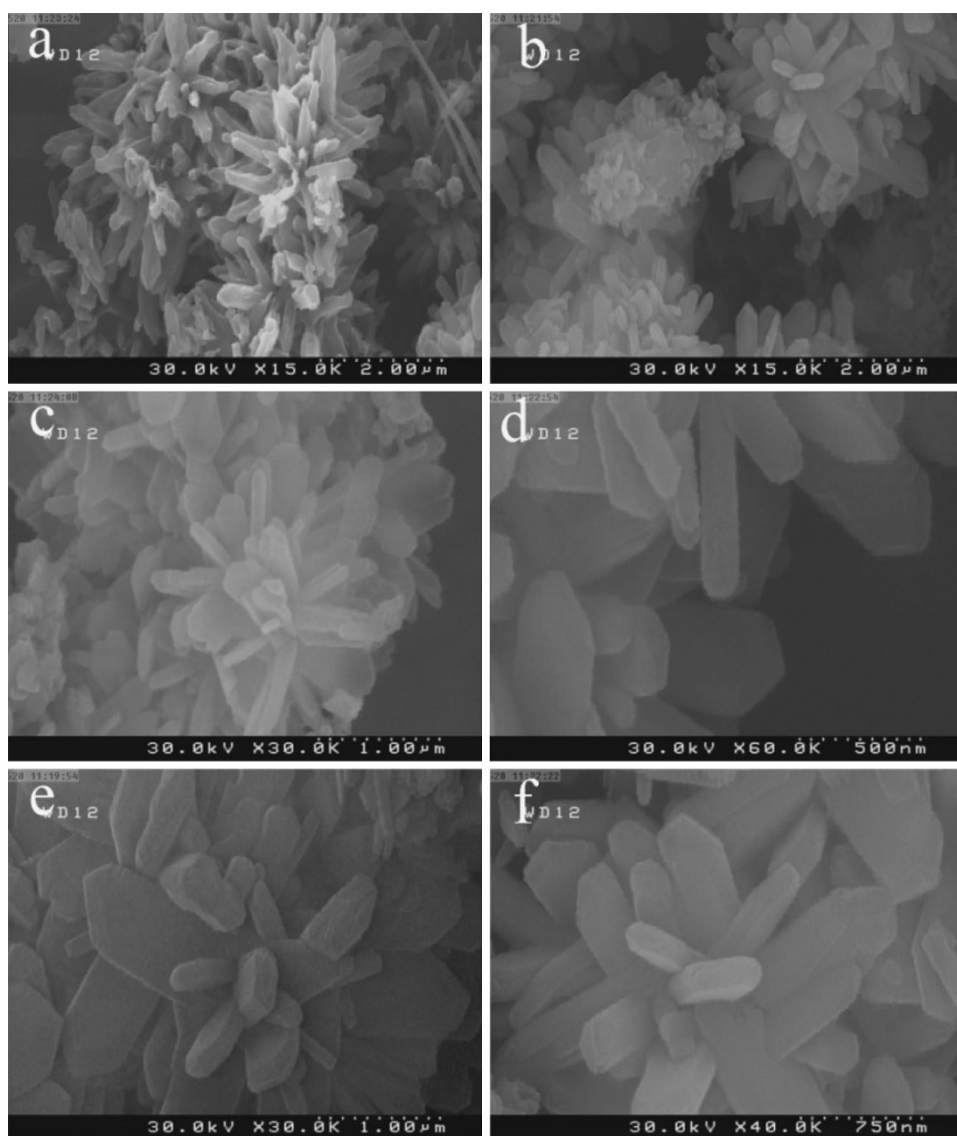


Table 2 Cell parameter refinement plot of Li_2SiO_3 showing a contraction along the *a*, *b*, and *c* directions in the unit cell

| | <i>a</i> | <i>b</i> | <i>c</i> |
|--------------------------------------|----------|----------|----------|
| Standard sample (pdf number:14-0322) | 9.3920 | 5.3970 | 4.6600 |
| Sample 1 | 9.3870 | 5.3988 | 4.6703 |
| Sample 2 | 9.3867 | 5.3990 | 4.6703 |
| Sample 3 | 9.3861 | 5.3983 | 4.6690 |

nearly homogenous morphology with of about 1 μm long and 300 nm wide and about 60 nm thick. The image in Fig. 2d, shows the high-magnification image of the obtained materials. It shows that there is another rod-like structure, where its length is about 500 nm and its width is about 70–80 nm.

Figure 3 represents the SEM images of the synthesized Li_2SiO_3 nanomaterials after 72 h at 180 °C. Figure 3

shows that after 72 h, the morphology of the obtained material is a mixture of rod- and belt-like structures, consisting of sheets with no regular edge shape. So, with increasing the reaction time from 48 h to 72 h, the morphology of the obtained materials has been changed to the a mixed structure. Figure 3a, b and d shows the rod-like structure of the as-prepared materials with no significant orientation. Figure 3c shows that there is another structure that is belt structure whose width is about 50–60 nm and its length (Fig. 3b) is about 2 μm . However, as shown in Fig. 3c, the whole sizes of the obtained materials synthesized at 72 h are nearly the same those of 48 h.

Figure 4 shows the FESEM images of the synthesized materials at 2:3 Li:Si molar ratio with lithium nitrate and silicon dioxide as raw materials at 96 h and 180 °C. With low magnification at Fig. 4a, b, it is clear that the obtained structures are in flower forms. From Fig. 4a, c and f, it can



Fig. 5 FTIR spectra of the synthesized Li_2SiO_3 nanomaterials, where (a) is at 48 h, (b) is at 72 h, and (c) is at 96 h

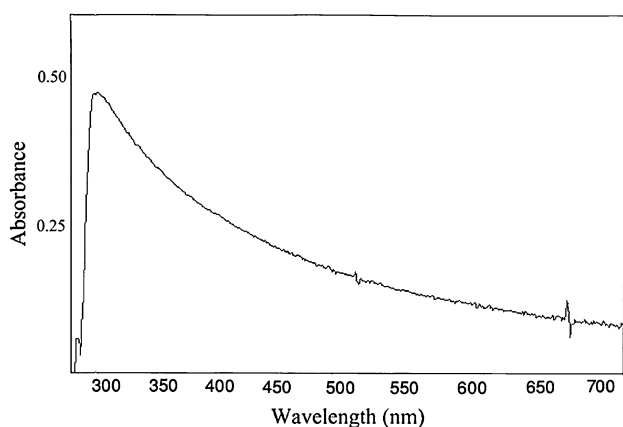
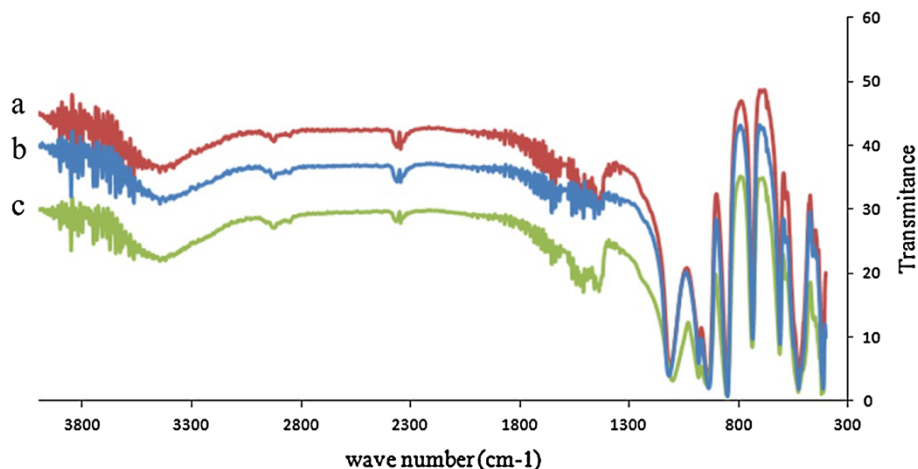


Fig. 6 UV-Vis spectra of the synthesized Li_2SiO_3 nanomaterials, where is at 96 h

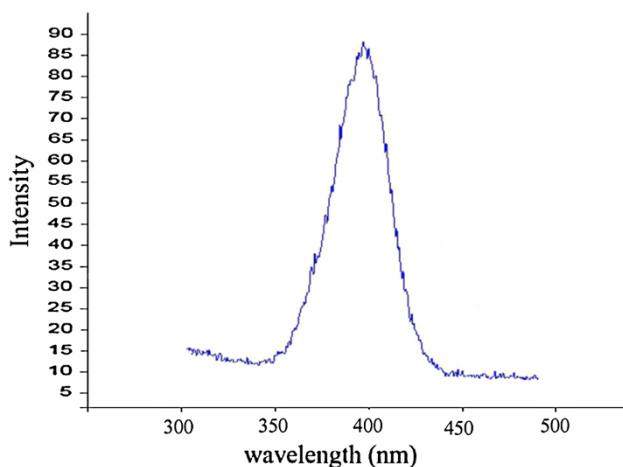


Fig. 7 Photoluminescence spectra of the synthesized Li_2SiO_3 nanomaterials ($\lambda_{\text{ex}} = 200 \text{ nm}$), where is at 96 h

be seen that there are three types of synthesized flower structures. From higher magnification at Fig. 4d and f, it is clear that the flowers are formed from the belt structures that

cut each other forming a flower structure. Also, the whole size of the flower is about 1–2 μm and as shown in Fig. 4d, its length is about 200–500 nm, its width is about 60–300 nm, and its thickness is about 50–70 nm. And from Fig. 4f, the length of the belt is about 300–600 nm, its width is 100–300 nm, and its thickness is about a minimum 70 nm and maximum 200 nm. At the end, it is clear that compared to Figs. 2 and 3, the obtained materials shown in Fig. 4 are significantly smaller than those shown in Figs. 2 and 3.

Table 2 shows the cell parameter refinement data of the as-synthesized nanomaterials. It is clear that parameters a and b values of the as-synthesized materials are smaller, and c value is larger than those of the standard sample. However, parameters a, b, and c for S_3 are smaller than those of S_1 . Also, in SEM images, we found that the particle morphology changed from a belt-like structure (S_1) to a flower-like structure (S_3), and the particle sizes of the S_3 are smaller than of S_1 ; so we conclude that parameters a, b, and c are the main factors on the size and the morphology of the materials [4]. And in agreement to debye–scherrer equation and SEM images, celref data show a contraction in unit cell for the materials at 96 h compared to 48 h as reaction time at 180 $^\circ\text{C}$.

Optical properties

Figure 5 shows the FTIR spectra of the obtained materials at different reaction times and at 180 $^\circ\text{C}$. The peaks at 420.65 and 523.30 cm^{-1} are assigned to deformation vibration; the peaks at 613.98, 733.00, 931.11, and 984.56 cm^{-1} are assigned to Si–O–Si and O–Si–O stretching vibration; the peaks at 1,112.92 cm^{-1} is assigned to Si–O stretching vibration; the peaks at 1,454.09, 1,509.51 and 1,644.65 cm^{-1} are assigned to C=O stretching vibration, and the peak at 3,447.49 cm^{-1} is assigned to O–H stretching vibration [21]. Also, the double peaks at around 2,600 cm^{-1} is assigned to KBr.

Figure 6 shows UV–Visible absorption spectrum of the pure phase Li_2SiO_3 powders produced by the hydrothermal reaction at 180 °C for 96 h. A sharp absorption band at 280, 283, and 288 nm is observed for samples a, b, and c, respectively. The band gap energy estimated from UV–Vis spectra is *ca.* 4.43, 4.38, and 4.30 eV.

Figure 7 represents the room-temperature emission spectra of the as-synthesized materials under excitation at 200 nm. A strong broad emission band at 423, 415, and 402 nm is observed for samples a, b, and c, respectively. So, there is a blue shift in the emission spectra with increasing the reaction time from 48 to 96 h.

Conclusion

In summary, uniform belt-, rod-, and flower-like lithium metasilicate were successfully synthesized by a simple hydrothermal method. We found that the reaction time has a major effect on the size and morphology of the products. However, the preferred crystallographic orientation of the crystals in the products changes with reaction time. UV–Vis electronic absorption and emission spectra of the synthesized materials were investigated. Also, cell parameter refinement was calculated by Celref software version 3.

Acknowledgments The authors express their sincere thanks to the authorities of Tabriz University for financing the project.

Open Access This article is distributed under the terms of the Creative Commons Attribution License which permits any use, distribution, and reproduction in any medium, provided the original author(s) and the source are credited.

References

- Du, J., Corrales, L.R.: Characterization of the structural and electronic properties of crystalline lithium silicates. *J. Phys. Chem.* **110**, 22346–22352 (2006)
- Beall, G.H.: Design and properties of glass-ceramics. *Annu. Rev. Mater. Sci.* **22**, 91–119 (1992)
- Vincent, C.A.: Lithium batteries: a 50-year perspective, 1959–2009. *Solid State Ion.* **134**, 159–167 (2000)
- Lu, C.H., Cheng, L.W.: Reaction mechanism and kinetics analysis of lithium nickel oxide during solid-state reaction. *J. Mater. Chem.* **10**, 1403–1419 (2000)
- Subramanian, V., Chen, C.L., Chou, H.S., Fey, G.T.K.: Microwave-assisted solidstate synthesis of LiCoO_2 and its electrochemical properties as a cathode material for lithium batteries. *J. Mater. Chem.* **11**, 3348–3353 (2001)
- Pfeiffer, H., Bosch, P., Bulbulian, S.: Sol–gel synthesis of $\text{Li}_2\text{ZrSi}_6\text{O}_{15}$ powders. *J. Mater. Chem.* **10**, 1255–1258 (2000)
- Pfeiffer, H., Bosch, P.: Thermal stability and high-temperature carbon dioxide sorption on hexa-lithium zirconate ($\text{Li}_6\text{Zr}_2\text{O}_7$). *Chem. Mater.* **17**, 1704–1710 (2005)
- Mosqueda, H.A., Vazquez, C., Bosch, P., Pfeiffer, H.: Nanoscale domain control in multiferroic BiFeO_3 thin films. *Chem. Mater.* **18**, 2307–2310 (2006)
- Pfeiffer, H., Vazquez, C., Lara, V.H., Bosch, P.: Thermal behavior and CO_2 absorption of $\text{Li}_{2-x}\text{Na}_x\text{ZrO}_3$ solid solutions. *Chem. Mater.* **19**, 922–926 (2007)
- Vinod, M.P., Bahnemann, D.: Materials for all-solid-state thin-film rechargeable lithium batteries by sol–gel processing. *J. Solid State Electrochem.* **7**, 493–498 (2002)
- Zhang, B., Easteal, A.J.: Effect of HNO_3 on crystalline phase evolution in lithium silicate powders prepared by sol–gel processes. *J. Mat. Sci.* **43**, 5139–5142 (2008)
- Cruz, D., Bulbulian, S., Lima, E., Pfeiffer, H.: Kinetic analysis of the thermal stability of lithium silicates (Li_4SiO_4 and Li_2SiO_3). *J. Solid State Chem.* **179**, 909–911 (2006)
- Nakazawa, T., Yokoyama, K., Noda, K.: Ab initio MO study on hydrogen release from surface of lithium silicate. *J. Nucl. Mat.* **258**, 571–574 (1998)
- Munakata, K., Yokoyama, Y.: Ab initio study of electron state in Li_4SiO_4 crystal. *J. Nucl. Sci. Technol.* **38**, 915–921 (2001)
- Taddia, M., Modesti, P., Albertazzi, A.: Determination of macro-constituents in lithium zirconate for tritium-breeding applications. *J. Nucl. Mat.* **336**, 173–191 (2005)
- Pfeiffer, H., Bosch, P., Bulbulian, S.: Synthesis of lithium silicates. *J. Nucl. Mat.* **257**, 309–316 (1998)
- van der Laan, J.G., Kawamura, H., Roux, N., Yamaki, D.: Ceramic breeder research and development: progress and focus. *J. Nucl. Mat.* **283**, 99 (2000)
- Cruz, D., Bulbulian, S.: Synthesis of Li_4SiO_4 by a modified combustion method. *J. Am. Ceram. Soc.* **88**, 1720–1724 (2005)
- Ortiz-Landeros, J., Contreras-García, M.E., Gómez-Yáñez, C., Pfeiffer, H.: Surfactant-assisted hydrothermal crystallization of nanostructured lithium metasilicate (Li_2SiO_3) hollow spheres: (I) Synthesis, structural and microstructural characterization. *J. Solid State Chem.* **184**, 1304–1311 (2011)
- Tang, T., Zhang, Z., Meng, J.B., Luo, D.L.: Synthesis and characterization of lithium silicate powders. *Fusion Eng. Des.* **84**, 2124–2130 (2009)
- Mohamed Mahmoud, M.: Crystallization of lithium disilicate glass using variable frequency microwave processing. April 24, (2007), Blacksburg, Virginia
- Alemi, A., Khademinia, S., Dolatyari, M., Bakhtiari, A.: Hydrothermal synthesis, characterization, and investigation of optical properties of Sb^{3+} -doped lithium silicates nanostructures. *Int. Nano Lett.* **2**, 20–29 (2012)
- Gutierrez, G.M., Cruz, D., Pfeiffer, H., Bulbulian, S.: Low temperature synthesis of Li_2SiO_3 : effect on its morphological and textural properties. *Res. Lett. Mat. Sci.* **2**, 1 (2008)
- Zhang, B., Allan, T.W., Easteal, J.: Effect of HNO_3 on crystalline phase evolution in lithium silicate powders prepared by sol–gel processes. *J. Mater. Sci.* **43**, 5139–5142 (2008)
- Alemi, A., Khademinia, S., Joo, S.W., Dolatyari, M., Bakhtiari, A.: Lithium metasilicate and lithium disilicate nanomaterials: optical properties and density functional theory calculations. *Int. Nano Lett.* **3**, 14–25 (2013)
- Ilyushin, G.D.: *Inorg. Mater.* **38**, 927–933 (2002)
- Zhao, T., Qin, Y., Zhang, P., Wang, B., Yang, J.F.: High-performance, reaction sintered lithium disilicate glass–ceramics. *Ceram. International.* **40**, 12449–12457 (2014)
- Alemi, A., Khademinia, S., Sertkol, M.: Part III: lithium metasilicate (Li_2SiO_3): mild condition hydrothermal synthesis, characterization and optical properties. Submitted manuscript. *Int. Nano Lett.* (2014)
- Alemi, A., Woo Joo, S., Khademinia, S., Dolatyari, M., Bakhtiari, A., Moradi, H., Saeidi, S.: Hydrothermal synthesis and characterization of straw bundle-like lithium sodium disilicate (silinaite) micro-rods. *Int. Nano Let.* **3**, 38–43 (2013)

